

УДК 532.526.4

UDC 532.526.4

**ТЕОРИЯ ТУРБУЛЕНТНОСТИ И
МОДЕЛИРОВАНИЕ ТУРБУЛЕНТНОГО
ПЕРЕНОСА В АТМОСФЕРЕ
ЧАСТЬ 5**

Трунев Александр Петрович
к. ф.-м. н., Ph.D.
Директор, A&E Trounev IT Consulting, Торонто,
Канада

Исследованы численные решения системы уравнений турбулентного преноса примесей в приземном слое атмосферы и для больших масштабов

Ключевые слова: АТМОСФЕРНАЯ
ТУРБУЛЕНТНОСТЬ, ТУРБУЛЕНТНЫЙ
ПЕРЕНОС, УСКОРЕННЫЕ ТЕЧЕНИЯ,
ПОГРАНИЧНЫЙ СЛОЙ, ШЕРОХОВАТАЯ
ПОВЕРХНОСТЬ, ПРИЗЕМНЫЙ СЛОЙ
АТМОСФЕРЫ, ТУРБУЛЕНТНЫЙ ПЕРЕНОС
АЭРОЗОЛЕЙ

**THEORY OF TURBULENCE AND
SIMULATION OF TURBULENT TRANSPORT
IN THE ATMOSPHERE
PART 5**

Alexander Trunev
Ph.D.
Director, A&E Trounev IT Consulting, Toronto,
Canada

Numerical solutions of equations system of turbulent transport of admixtures in a surface layer of the atmosphere and for a large scale have been studied

Keywords: ACCELERATED FLOW, AEROSOL
TURBULENT TRANSPORT, ATMOSPHERIC
STRATIFIED FLOW, ATMOSPHERIC
TURBULENCE, ATMOSPHERIC SURFACE
LAYER, BOUNDARY LAYER, ROUGH
SURFACE, TURBULENT TRANSPORT

5. Turbulent transport in the atmospheric surface layer

5.1. Model of turbulent transport in the stratified surface layer

The mathematical models of the turbulent transport in the atmospheric surface layer are widely used in meteorology and for the urban air quality forecast [2-32, 37-38, 44-48]. The finite element modelling of plume dispersion in the stratified surface layer has been developed by Pugliese et al [119] based on the Monin-Obuchov similarity theory [21-22] and $k - e$ model which has been modified for geophysical applications by Rodi [126-127]. The turbulent flow in the street canyon has been considered by Hassan & Crowther [128] and other. The turbulent flow and the air pollutants dispersion in the Central London has been estimated by Ni Riain et al [12].

Numerical solutions of equations system of turbulent transport of admixtures in a surface layer of the atmosphere for a large scale have been studied in this paper. An equation of the model of turbulent diffusion in a stratified boundary layer has been deduced. An expression of deposition velocity of gas admixtures and aerosols in the stratified flows has been obtained. It has been shown that in a case of stable or neutral stratification the deposition velocity depends mainly on dynamic velocity. In the case of unstable stratification the deposition velocity depends on a parameter of stability that is well conform to data of natural experiments. On the base of developed models, numerical research of admixtures transport into the areas, possessing several highways has been performed. Application of the results obtained to the air pollution modelling in Sochi (Russia) has been considered [2, 13-14]. Equations of dusty turbulent boundary layer have been deduced. In the dynamic equations of dusty gas, a diffusion of parti-

cles has been taken into consideration owing to their Brownian motion as well as a velocity of particles generation, in a type of aerosols, during a process of a vapour phase condensation. The problem of particles' diffusion over industrial area with a prescribed value of emission has been considered. An exact solution of a task has been obtained with a prescribed value of emission in a kind of periodic function by which a daily rhythm of waste produced by traffic and enterprises is being modelled. Qualitative conformation of the solutions obtained to the data of experiments is emphasized.

The turbulence theory developed in the previously sections can be used to estimate the turbulent transport in the atmospheric surface layer. Let us consider the solutions of the equation system (2.10) at the large distance from the wall. In this case the main parameter characterized the turbulent flow is the streamwise velocity $y = u^+$. Using the new variable $V = I \operatorname{Arsh}(z/I)$ the equation system (2.10) can be transformed as follows:

$$\begin{aligned} \frac{\partial y}{\partial t} + \frac{W}{\operatorname{ch}(V/I)} \frac{\partial y}{\partial V} &= n \frac{\partial^2 y}{\partial V^2} \\ \frac{\partial \tilde{T}}{\partial t} + \frac{W}{\operatorname{ch}(V/I)} \frac{\partial \tilde{T}}{\partial V} &= \frac{n}{\Pr} \frac{\partial^2 \tilde{T}}{\partial V^2} \\ \frac{\partial \tilde{f}}{\partial t} + \frac{W}{\operatorname{ch}(V/I)} \frac{\partial \tilde{f}}{\partial V} &= D \frac{\partial^2 \tilde{f}}{\partial V^2} \end{aligned} \quad (5.1)$$

To close the system (5.1) we can use the equation (2.13) written in the inner layer variables, thus

$$\begin{aligned} \frac{\partial^2 W^+}{\partial x \partial t} + W^+ \frac{\partial^2 W^+}{\partial x^2} - \frac{1}{I^+} \frac{\partial}{\partial x} (1+x^2) \frac{\partial^2 W^+}{\partial x^2} &= \\ = \frac{x}{1+x^2} \frac{\partial W^+}{\partial t} + \frac{b_0 x (\tilde{r}/r_0 - 1)}{1+x^2} & \end{aligned} \quad (5.2)$$

where $W^+ = \tilde{W}/u_*$, $b_0 = I g/u_*^2$.

In case of a neutral stratification for $z \gg I$ the contribution of the vertical velocity in the turbulent transport is so small value that can be neglected. Therefore the equation system (5.1) can be simplified and rewritten in the classical diffusion equation form:

$$\begin{aligned} \frac{\partial y}{\partial t} &= n \frac{\partial^2 y}{\partial V^2} \\ \frac{\partial \tilde{T}}{\partial t} &= \frac{n}{\Pr} \frac{\partial^2 \tilde{T}}{\partial V^2}, \quad \frac{\partial \tilde{f}}{\partial t} = D \frac{\partial^2 \tilde{f}}{\partial V^2} \end{aligned} \quad (5.3)$$

In the boundary layer the general solution of the equation system (5.3) can be expressed as a linear function of the variable V ,

$$y = a_1 + b_1 V, \quad \tilde{T} = a_2 + b_2 V, \quad \tilde{F} = a_3 + b_3 V, \quad V \approx I \ln(2z/I),$$

where the parameters a_i, b_i , can be estimated from the solution of the inner layer problem or from the experimental data.

As it follows from the equation system (5.3) and from the boundary layer solutions, the molecular transport parameters (for example, the kinematic viscosity) have a sense only in the non-stationary turbulent flow, and in the steady-state flow the molecular transport parameters fall out from the problem. It should be noted, that the main experimental data has been obtained for the steady-state turbulent flows, in which the universal logarithmic profile of the mean velocity and temperature has been established. According to the equations (5.2) the molecular transport parameter effect can be found in the turbulent flow, the mean velocity of which vary in time or in space rather quickly. For instance, in the turbulent flow in pressure gradient, as it was established in the previous chapter, the dimensionless acceleration parameter is direct proportional to the molecular viscosity, i.e., $g_*^+ = \frac{n}{ku_*^3} U_0 \frac{\partial U_0}{\partial x}$.

The model of turbulent transport in the stratified surface layer can be derived from the equation system (5.1). As it has been shown in the section 4.2 there is $\lim_{x \rightarrow \infty} j(x) = j_0(B)$, where $j_0(B)$ is a function of the stability parameter. Practical we have $j(x) \approx j_0(B)$ for $x \geq x_0$, where $x_0 \approx 10^2$. Therefore for $x \gg x_0$: $W^+ = W_0^+ - j_0(x - x_0)$, $W_0^+ = W^+(x_0)$, hence the first equation (5.1) can be rewritten as

$$\frac{\frac{dy}{dt}}{\frac{dy}{dV}} + \Delta W \frac{\frac{dy}{dt}}{\frac{dy}{dV}} = n \frac{\frac{d^2y}{dV^2}}{\frac{dy}{dV}} \quad (5.4)$$

where $\Delta W = -u_* j_0(B)$.

In the steady-state turbulent flow, when $y \approx u^+$, the first integral of the equation (5.4) is given by

$$\Pi_1 = kl^+ \Delta Wu - K_z \frac{\frac{du}{dz}}{\frac{dy}{dz}} \quad (5.5)$$

Here $\Pi_1 = u_*^2$ is the momentum turbulent flux in the surface layer, $K_z = ku_* z$ is the standard vertical diffusion coefficient in the neutral stratified turbulent flow.

Consequently the turbulent heat flux can be written as follows

$$\frac{\Pi_T}{rc_p T_*} = kl^+ \Delta WT^+ - K_z \frac{\partial T^+}{\partial z} \quad (5.6)$$

where $\Pi_T = rc_p u_* T_*$ is the turbulent heat flux in the surface layer, $I_T^+ = I_0^+ (1 + 0.217 \ln \text{Pr}) / \text{Pr}$. Note, that for the atmospheric flows the Prandtl number is about $\text{Pr} \approx 0.7$.

In the case of the impurity turbulent transport we can suppose that the impurity concentration turbulent flux has a constant value in the surface layer (the Monin-Obuchov similarity theory)

$$\Pi_f / f_* = k l_f^+ \Delta W f^+ - K_z \frac{\partial f^+}{\partial z} \quad (5.7)$$

where $\Pi_f = u_* f_*$ is the turbulent impurity concentration flux, f_* is the impurity concentration turbulent scale, $I_f^+ = I_0^+ (1 + 0.217 \ln(\text{Sc})) / \text{Sc}$. Integrated the equation (5.7) we have the impurity concentration profile in the stratified turbulent flow as follows

$$f = \frac{\Pi_f}{k l_f^+ \Delta W} + \left(f_g - \frac{\Pi_f}{k l_f^+ \Delta W} \right) \exp \left(\frac{I_f^+ \Delta W}{u_*} \ln \frac{z_1}{z_0} \right)$$

where $f_g = f(z_0)$ is the impurity concentration for $z = z_0$.

The important parameter, widely used in the environmental problems, is the deposition velocity which can be defined as $u_d = \Pi_f / f_g$. Practically to estimate the deposition velocity we can use the impurity concentration profile for $z_1 = H$, then we have

$$u_d = \frac{\Pi_f}{f_g} = k l_f^+ \Delta W \frac{\bar{f}_0 - \exp \left(\frac{I_f^+ \Delta W}{u_*} \ln \frac{H}{z_0} \right)}{1 - \exp \left(\frac{I_f^+ \Delta W}{u_*} \ln \frac{H}{z_0} \right)} \quad (5.8)$$

where $\bar{f}_0 = f(H) / f_g$, H is the boundary layer height.

In the case of the neutral and slow stable stratification when $\Delta W \rightarrow 0$ we have from (5.8) $u_d = k u_* (\bar{f}_0 - 1) / \ln(H / z_0)$, thus the deposition velocity depends mainly on the turbulent velocity scale u_* .

In the case of the unstable stratification the deposition velocity mainly depends on the vertical velocity ΔW which increases when the parameter $B = n / (u_* k L)$ decreases. The deposition velocity equation (5.8) is in a good agreement with the experimental data by Labatut et al [129] - see Figure 5.1. The solid lines shown in Figure 5.1 have been computed on (5.8) for $\text{Sc} = 0.8$ (ozone) and for $\text{Sc} = 2.15$ (sulphur aerosol) and for the typical range of the turbu-

lent velocity scale as well as for $u_* = 0.36 \text{ m/s}$ and for the typical range of the aerosols Schmidt numbers.

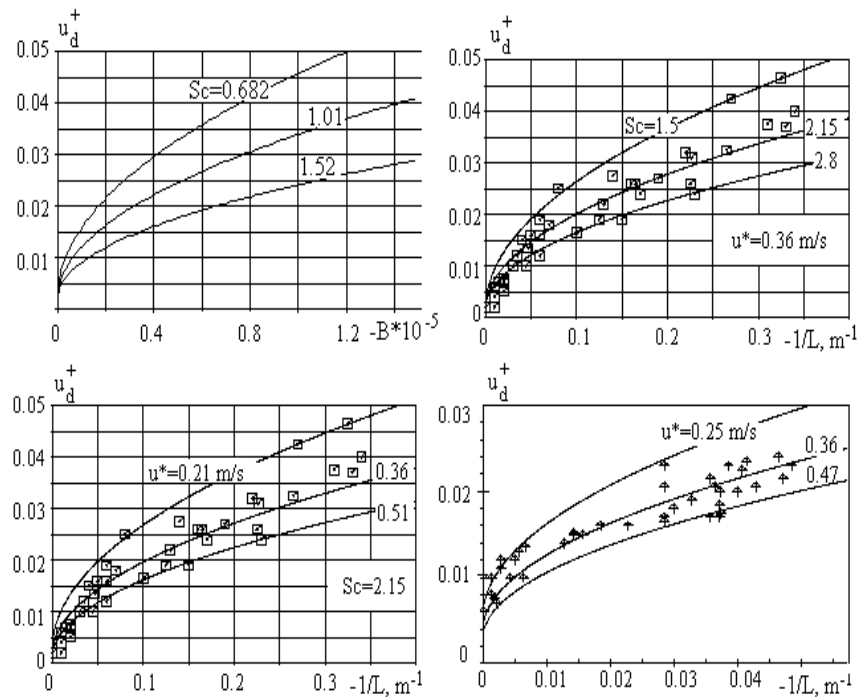


Figure 5.1: The deposition velocity versus the stability parameter for the unstable stratified flows. The solid lines are computed on (5.8). The experimental data for the sulfur aerosols by Labatut et al [129] are shown by the square symbols. The ozone deposition data [129] are shown in the right bottom part

5.2. Numerical modelling of air pollutants turbulent transport in region with several roads

5.2.1. Turbulent transport model description

The model of the turbulent transport in the atmospheric surface layer over the region with several roads can be derived from the third equation (5.1) as follows

$$\frac{\partial C}{\partial t} + U_x \frac{\partial C}{\partial x} + U_y \frac{\partial C}{\partial y} + k l_f^+ \Delta W \frac{\partial C}{\partial z} = \frac{\partial}{\partial z} K_z \frac{\partial C}{\partial z} \quad (5.9)$$

where $C(t, x, y, z) = \langle f \rangle$ is the mean impurity concentration, U_x, U_y are the wind velocity component profiles, ΔW is the mean velocity of the vertical transport produced by the buoyancy forces in the stratified flow, $K_z = k u_* z$ is the standard turbulent transport parameter, $k = 0.41$ is the Karman constant, u_* is the

turbulent velocity scale (the friction velocity), $I^+ = 8.71(1 + 0.217 \ln(Sc)) / Sc$, $Sc = n / D$ is the Schmidt number calculated on the molecular diffusion parameter and the air kinematic viscosity.

The mean vertical transport dimensionless parameter depends on the stability parameter as

$$\Delta W^+ = \begin{cases} -2.85(-B)^{\frac{1}{2}}, & L < 0 \\ 19.93B^{\frac{1}{2}}, & L > 0 \end{cases} \quad (5.10)$$

$\Delta W^+ = \Delta W / u_*$, $B = n / (u_* k L)$, $L = -u_*^3 r c_p T_0 / (k g q_H)$ is the Monin-Obuchov stability parameter.

In case of the spatial homogenous, stable-state turbulent flow the wind velocity profile can be estimated from the equations system (4.11) rewritten for this case as follows:

$$\begin{aligned} \frac{dc}{dx} &= j, \\ (1+x^2) \frac{d^2j}{dx^2} + (I_0^+ c + 2x) \frac{dj}{dx} &= -B_0 \frac{x I_0^{+2} T^+}{1+x^2} \\ \frac{du^+}{dz^+} &= \frac{e^{-I}}{\sqrt{1+(z^+/I_0^+)^2}}, \\ \frac{dT^+}{dz^+} &= \frac{\Pr \exp[-\Pr I_T^+ I_1 - \Pr I_T^+ (1-\bar{I}) I_2]}{\sqrt{1+(z^+/I_T^+)^2}} \end{aligned} \quad (5.11)$$

$I_T^+ = I_0^+ (1 + 0.217 \ln \Pr) / \Pr$ is the turbulent length scale of the thermal layer, $\bar{I} = I_T^+ / I_0^+$, $x = z^+ / I_0^+$, $x_l = z^+ / I_T^+$; \Pr is the Prandtl number; $I_0^+ = 8.71$ is the main turbulent length scale,

$$I = \int_0^x \frac{I_0^+ c dx}{1+x^2}, \quad I_1 = \int_0^{x_l} \frac{c(\bar{I}x) dx}{1+x^2}, \quad I_2 = \int_0^{x_l} \frac{j(\bar{I}x) x dx}{1+x^2}.$$

The buoyant force parameter depends on the type of stratification and stability parameter as follows

$$B_0 = \begin{cases} B, & L < 0 \\ 41.85B, & L > 0 \end{cases}$$

Note that the stable and unstable stratified flows are realized at the positive and negative values of the stability parameter $B = n / (u_* k L)$ accordingly.

The boundary conditions on the effective smooth surface can be written as follows

$$x = 0: \quad c(0) = T^+(0) = u^+(0) = 0, \quad j(0) = w_0^+ \quad (5.11,a)$$

In the outer region of the turbulent boundary layer in a case of the unstable stratification we have

$$\lim_{z^+ \rightarrow \infty} u^+(z^+) = u_\infty^+(B), \quad \lim_{z^+ \rightarrow \infty} T^+(z^+) = T_\infty^+(B) \quad (5.11,b)$$

where $u_\infty^+(B), T_\infty^+(B)$ are functions of the stability parameter.

In a case of unstable stratification the boundary conditions are set as follows

$$z = L: \quad u^+ = u^+(L), \quad T^+ = T^+(L) \quad (5.11,c)$$

Here functions $u^+(L), T^+(L)$ can be defined, for instance, from experimental data.

The wind velocity profile and the vertical turbulent transport rate are dependent on the stability parameter in the stratified flows. The Monin-Obuchov stability parameter depends on the heat flux as $L = -u_*^3 r c_p T_0 / (k g q_H)$, and consequently the heat flux must be determined as an input parameter. In the daytime it can be considered as some function of the solar radiation flux. Thus the heat flux on the ground surface in a daytime is modeled as a function of the angle of incidence and the clouds coverage as follows (see [27,130]):

$$K^* = (990 \cos \Theta - 30)(1 - 0.75 N_{cl}^{3.4})(1 - R_a)$$

$$q_H = 0.4(K^* - 91 + 60N_{cl})$$

Here Θ is the angle of incidence of the solar radiation on the horizontal surface, N_{cl} is the cloud coverage factor (in the numerical model this factor has been estimated as $N_{cl} = 0.3$), $R_a = 0.2$ is the ground surface albedo parameter, $q_H [W/m^2]$.

The angle of incidence is computed on the standard formula given by Paltridge & Platt [130]:

$$\cos\Theta = \sin d \sin j_e + \cos d \cos j_e \cos \hat{f}$$

$$d = 0.006918 - 0.399912 \cos J + 0.070257 \sin J -$$

$$- 0.006758 \cos 2J + 0.000907 \sin 2J -$$

$$- 0.002697 \cos 3J + 0.001480 \sin 3J$$

$$J = 2pt_y / \Delta t_y, \hat{f} = 2pt / \Delta t_d$$

where j_e is the latitude, $t_y, \Delta t_y$ are time in days and the astronomical year period, t_d is the astronomical day period. Note that the daily time is counted from the astronomical noon.

5.2.2. Turbulent transport over the region with several parallel roads

As applied result the problem of impurity diffusion over the region with several parallel roads has been numerically solved. It was suggested that the roads are separated by the buildings and that the wind direction is perpendicular to the roads lines. Note that in the case when the wind velocity vector has a component along the roads, then one can put in the equation (5.9) $U_x = U_0 \sin g_0$, where U_0 is the wind speed profile, g_0 is the angle between the wind velocity vector and the road line.

The co-ordinates system chosen for the turbulent transport modelling is shown in Figure 5.2. The vertical axis OZ is directed opposite to the gravity acceleration vector, and the horizontal axis OX is parallel to the wind velocity vector.

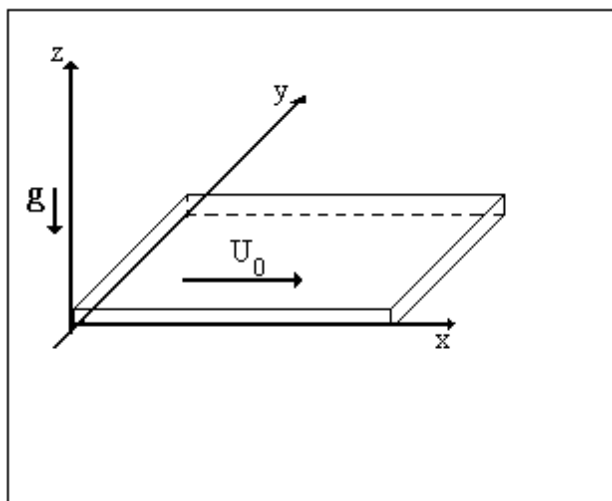


Figure 5.2: The coordinate system chosen for the turbulent flow description

Usually the mean motor transport emission rate depends on the traffic rate, which slowly varies with time, as, for instance, the hourly averaged temporal variations of traffic flow rate (vehicles per hour) on the Kurortny Avenue of the Central Sochi (Russia) in the daytime (August, 1998) which is shown in Figure 5.3. Therefore in this problem the impurity concentration can be considered as a function of two variables, $C = C(x, z)$, and consequently the turbulent transport equation (5.9) can be rewritten in the form

$$\cdot U_x \frac{\partial C}{\partial x} + k l_f^+ \Delta W \frac{\partial C}{\partial z} = \frac{\partial}{\partial z} K_z \frac{\partial C}{\partial z} \quad (5.12)$$

Using the general theory of the parabolic equations we can consider only the region of a solution of equation (5.12) in which $U_x > 0$. Hence, put $U > 0$ for $x > 0$ in (5.12), then the boundary conditions for the equation (5.12) can be set as follows:

$$x = 0: C(z) = 0; \quad x > 0: \lim_{z \rightarrow \infty} C(z) = 0 \quad (5.12')$$

$$x > 0; z = z_0: J = J_i \text{ for } x_i < x \leq x_i + l_i;$$

$$J = k l_f^+ \Delta W C(z_0) \text{ for } x_i + l_i \leq x < x_{i+1},$$

Here $x_i < x \leq x_i + l_i$ is the region of the road with a number i ; $x_i + l_i \leq x < x_{i+1}$ is the region between two roads; l_i is the width of the road with a number i .

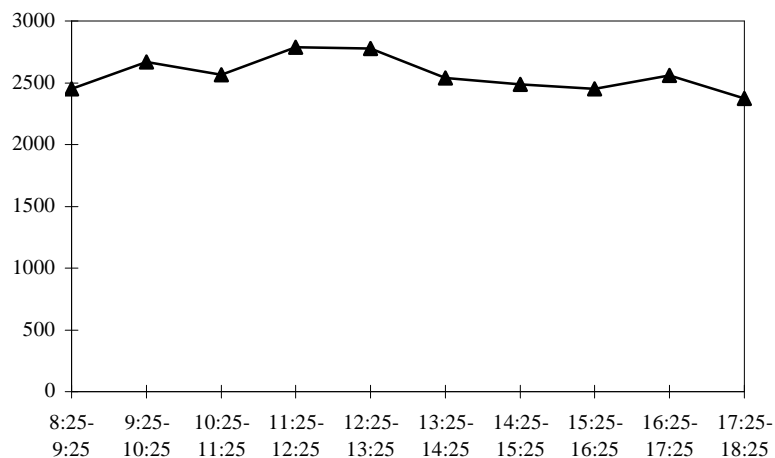


Figure 5.3: Hourly averaged temporal variations of traffic flow rate (vehicles per hour) on the Kurortny Avenue of the Central Sochi in the daytime (August, 1998)

Put the new variables: $\tilde{x} = x / l_1$, $z = \ln(z / z_0)$, where $l_1 = l_R$ is the width of the first road. Multiplying both parts of the equation (5.12) on z and making the elementary transformations we have

$$\frac{u^+ z_0 e^V}{l_R} \frac{\frac{dC}{d\tilde{x}}}{\frac{dV}{d\tilde{x}}} + \frac{\frac{dJ^+}{dV}}{\frac{dV}{d\tilde{x}}} = 0, \quad J^+ = k l^+ \Delta W^+ C - k \frac{\frac{dC}{dV}}{\frac{dV}{d\tilde{x}}} \quad (5.13)$$

Let us consider the numerical method for the problem (5.12')-(5.13) solution. The discrete variables can be defined from the recurrent formulas as follows: $\tilde{x}_{k+1} = \tilde{x}_k + h_x$, $V_{n+1} = V_n + h_V$, where h_x, h_V are the steps of the grid. Consequently the grid functions depend on the discrete variables as

$$C_{k,n} = C(\tilde{x}_k, V_n), \quad J^+_{k,n} = J^+(\tilde{x}_k, V_n), \quad u_n^+ = u^+(V_n).$$

Therefore the discrete model of the equation system (5.13) can be written in the form

$$\begin{aligned} \frac{u_n^+ z_0 e^{V_n}}{l_R} \frac{C_{k+1,n} - C_{k,n}}{h_x} + \frac{J^+_{k,n+1} - J^+_{k,n}}{h_V} &= 0, \\ J^+_{k,n} &= k l^+ \Delta W^+ C_{k,n} - k \frac{C_{k,n} - C_{k,n-1}}{h_V} \end{aligned} \quad (5.14)$$

The explicit numerical solution of the equation system (5.14) is computed step by step in the mesh points $\tilde{x}_{k+1} = \tilde{x}_k + h_x$ as

$$C_{k+1,n} = C_{k,n} - \left(\frac{u_n^+ z_0 e^{V_n}}{l_R} \frac{1}{h_x} \right)^{-1} \frac{(J^+_{k,n+1} - J^+_{k,n})}{h_V} \quad (5.15)$$

The stability condition of the explicit numerical algorithm (5.15) depends on the grid steps as follows

$$h_x < e_{Num} \left(\frac{u_1^+ z_0}{2l_R k} \right) h_V^2$$

Here $e_{Num} \leq 1$ is the numerical algorithm stability parameter. This parameter has been estimated in the numerical experiments as $e_{Num} = 0.8$.

The numerical data for the carbon monoxide turbulent transport in the region with two parallel roads is shown in Figure 5.4. The road widths equals to ten meters, $l_1 = l_2 = 10$ m. The distance between the roads is about 100 meters. The traffic flow rates for both roads are put the uniform value, therefore the emission rate $J_1 = J_2$. The mean concentration of CO has been normalized on the turbulent scale of concentration used the emission rate of the first road, $C^* = J_1 / u_*$.

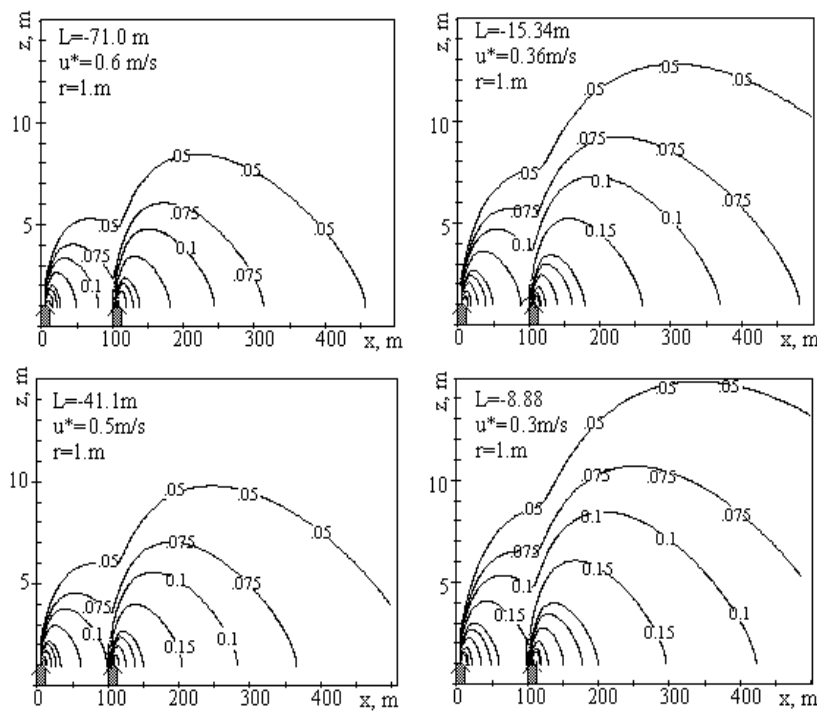


Figure 5.4: The normalized carbon monoxide concentration isolines in the turbulent unstable stratified flow over the region with two parallel roads located as it shown by the black pointers

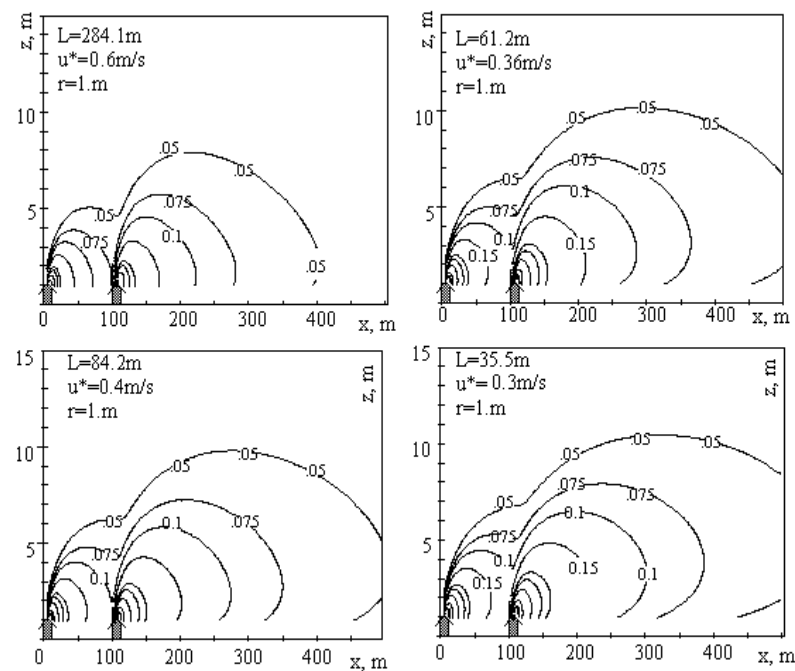


Figure 5.5: The normalized carbon monoxide concentration isolines in the turbulent stable stratified flow over the region with two parallel roads located as shown by the black pointers

The lines of equal concentration are given in Figure 5.4 in the unit of the turbulent scale C^* . The roughness length scale for the urban complex terrain is estimated as $r \approx 1\text{ m}$. The heat flux has been calculated as for the summer cloudless day, one hour before noon. Consequently the meteorological parameters are set as for the unstable stratification.

Figure 5.4 shows that the carbon monoxide cloud becomes more concentrated when the turbulent velocity scale decreases from $u_* = 0.6 \text{ m/s}$ down to $u_* = 0.3 \text{ m/s}$. As it has been established by Jenkins et al [131] the roadside air pollutants concentration is proportional to the traffic volume or emission rate and inversely proportional to the wind speed. This experimental result can be explained by the fact that the turbulent transport model (5.9) is a linear equation and therefore the turbulent scale of the impurity concentration can be estimated as $C^* = J_1 / u_*$.

In case of the stable stratification the vertical air pollutants turbulent transport rate is more intensive in comparison with the unstable stratified flow and directed up. Thus the cloud of carbon oxide impurity spreads up at the large distance from the roads - see Figure 5.5. Note that in this case also the impurity concentration increases when the turbulent velocity scale decreases.

5.2.3. Air pollutants turbulent transport in Central Sochi

The Central Sochi part shown in Figure 5.6 has been considered as applied example for the model (5.12)-(5.12') to estimate the air quality near the main streets. The computational square domain in the plane XZ intersects the main streets Kurortny Avenue and Ordgonikidze Street which are situated parallel to the Black Sea shoreline - see Figure 5.6. The predominate atmospheric boundary layer flow in the summer daytime is the breeze circulation. So, the wind direction is primary from the sea to the mountains, perpendicular to the street lines.

The data base of the meteorological parameters in the Sochi region, considered by Amirchanov *et al* [2], consists of the data set series for more than 100 years of the routine daily observations. The topography of the Sochi region includes the erosive relief and the rivers grid, the forest coverage, and the large difference of altitudes from the Black Sea level up to greatest altitude of 3256 m in the Caucasus Mountains. In the urban domain there are numerous buildings that also it is necessary to take into consideration in the model of the air pollution transport in the lower part of atmosphere. The air pollutants emission data base for the Sochi region has been discussed in [2,13-14,132]. As it has been established the main air pollution problem in this region is connected with the motor transport emission [14]. Therefore the process of turbulent diffusion of traffic wastes is localised in the surface layer of atmosphere and greatly depends on pa-

rameters of turbulence as well as on the condition of stratification. Also the roughness of ground surface, including the artificial roughness in a form of buildings, trees, etc [16] is a very important factor in this problem. The traffic flow and emission rate has been estimated for two main streets: Kurortny Avenue and Ordgonikidze Street. In summer daytime the traffic flow rate is about 1500 vehicles per hour for each of them in the cross section chosen for the air quality modelling.

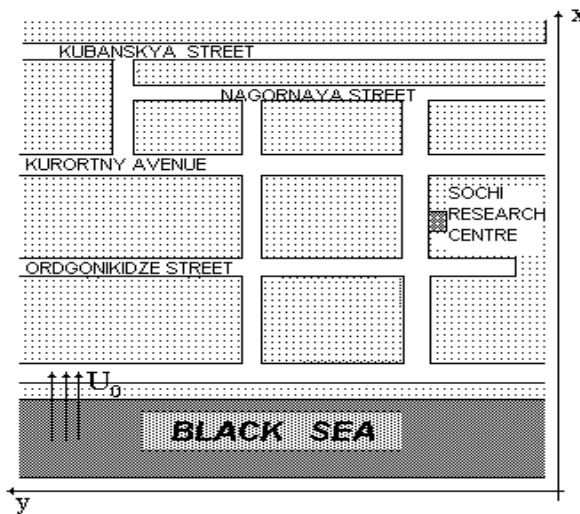


Figure 5.6: Central Sochi part geometry. The computational domain chosen for an estimation of the air pollutants turbulent transport is parallel to XZ plain, and intersects the main streets in the wind direction

It's known the carbon oxide and NO_x the main air pollutants which are dangerous for human. In the Central Sochi region the major sources of emission of CO and NOx are the gasoline passenger cars (>95%) [13]. The normal emission of CO is about 16 g/km in the urban region and about 30.4 g/km for the cold start. Hence the mean value of CO emission rate has been estimated as 19 g/km.

Put \tilde{q}_{CO} is the CO emission rate for one car, N_t^i is the traffic flow rate (=the number of cars going on the road cross section in the unit of time). Then the total emission rate can be estimated as $q_{CO}^i = \tilde{q}_{CO} N_t^i / l_i$.

Thus in the considered case the CO total emission rate is about $q_{CO}^i = 8 * 10^{-4} gs^{-1} m^{-2}$. This value has been used to compute the local zone in which the CO concentration is higher then the maximum permissible concentration.

The state sanitary standard adopted in Russia is the maximum permissible concentration (MPC) which in the case of CO emission is defined as $C_{MPC} = 5 \text{ mg/m}^3$.

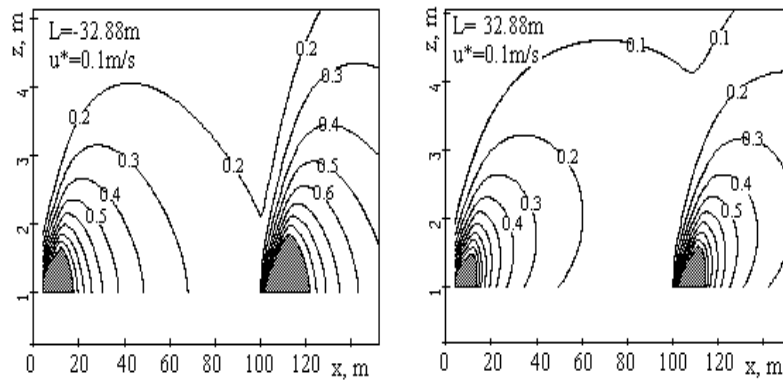


Figure 5.7: The isolines of CO concentration normalized on MPC in the turbulent stable (right) and unstable (left) stratified flow over the region with two parallel roads. Zones of the CO concentration over MPC are darkened

The isolines of CO concentration normalized on MPC are shown in Figure 5.7 for the stable (right) and unstable (left) stratification. The heat flux is computed for the cloudless sunset time. The roughness length is estimated for the urban landscape as $r \approx 1 \text{ m}$. Figure 5.7 shows that the dangerous zones of CO concentration can be near the roads (about 20 m from the roadside) due to the small value of the turbulent intensity in the evening time.

The turbulent transport of NO and NO_2 has been calculated for the daytime and evening time - see Figure 5.8. In this case the normal gasoline car emission rate is about 2 g/km, and for the passenger diesel it can be up to 12 g/km. Using the gasoline car emission rate the total emission rate of nitrogen oxides for the Kurortny Avenue can be estimated as $q_{NO_x}^i = 8.4 * 10^{-5} \text{ gs}^{-1} \text{ m}^{-2}$.

The maximum permissible concentrations for the nitrogen oxides is much less than for the carbon monoxide, it's only $C_{MPC} = 0.04 \text{ mg/m}^3$ for NO_2 , and $C_{MPC} = 0.06 \text{ mg/m}^3$ for NO.

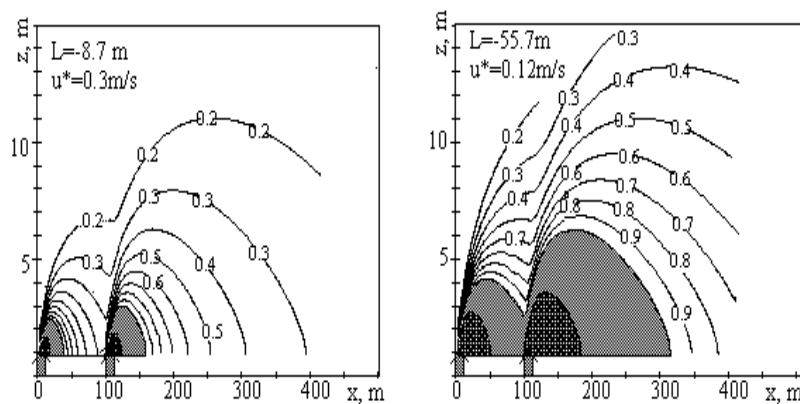


Figure 5.8: The isolines of NO_x concentration normalized on MPC in the turbulent unstable (right) and stable (left) stratified flow over the region with two parallel roads located as shown by the black pointers. Zones of NO_x concentration over MPC are darkened. In the black zones the NO_x concentration in two times higher than MPC

The turbulent transport data of NO_x concentration normalized on MPC computed for the day time (left) and evening time (right) are shown in Figure 5.8. This data shows that the dangerous zones in the evening time occupy the region which has the width about 300 m, and the height up to 6 m. Therefore the dangerous zones of NO_x concentration can occupy the habitable buildings as well as the kindergarten and musical school built near the considered roads cross section. Thus the nitrogen oxides can be one of the human health damaging factors in Sochi.

5.2.4. Turbulent transport of lead aerosols in Central Sochi

The lead aerosol is the most important damaging factor of the human health. The leaded gasoline has been widely used in the Sochi region. The lead concentration in the fuel dependent on the gasoline type varies from 170 up to 370 mg/l. The mean lead emission is estimated as $\tilde{q}_{pb} = 15 \div 33 \text{ mg/km}$. For the mean vehicle way per year about 30000 km it gives approximately 1 kg of the lead aerosol emitted by one normal passenger car. This value often has been used for the estimation of the lead aerosol effect on the biosphere [133].

The number of vehicles in the Sochi region has extremely grown in the last decade: from about 20000 in 1990 up to 100000 in 1999. The lead aerosol emission averaged on 10 years interval is 60 ton/ year. The total emission rate of lead aerosols for the Kurortny Avenue and Ordgonikidze Street in the modeled cross section is estimated as $q_{pb}^i = (0.5 \div 15) \text{ mgs}^{-1} \text{ m}^{-2}$.

The main difference between the gaseous pollutants and lead aerosols is that the lead can be accumulated by the top layer of soil. The maximum permissible

concentration of the lead in the air is not more than 0.0003 mg/m^3 , and on the ground - 250 mg/kg .

The turbulent transport of the lead aerosol in the region with parallel roads can be considered on the base of the model (5.13). The vertical turbulent transport rate in a case of the heavy particles can be estimated as for the gaseous pollutant transport but with the factor of the gravitational sedimentation. Thus the proposed model can be written as follows

$$\frac{u^+ z_0 e^V}{l_R} \frac{\nabla C}{\nabla x} + \frac{\nabla J^+}{\nabla V} = 0 , \quad (5.16)$$

$$J^+ = (-g t_p / u_* + k l^+ \Delta W^+) C - k \frac{\nabla C}{\nabla V}$$

Here $t_p = \frac{r_{pb}}{r_0} \frac{d^2}{18n}$ is the gravitational sedimentation time scale, $r_{pb} = 11373 \text{ kg/m}^3$ is the lead density in the solid condition, d is the particle diameter dependent on the condensation and crystallization rates.

The aerosol Schmidt number is estimated on the Brownian diffusion parameter as (see [48])

$$Sc = \frac{n}{D_p} = \frac{3prn^2 d}{kT}$$

where $k = 1.38 \cdot 10^{-23} \text{ joule/K}$ is the Boltzmann constant.

The boundary conditions can be written in the form (5.12') but with additional term counted the gravitational sedimentation, thus

$$x = 0: C(z) = 0 ; \quad x > 0: \lim_{z \rightarrow \infty} C(z) = 0 \quad (5.17)$$

$$x > 0; z = z_0: \quad J = J_i \text{ for } x_i < x \leq x_i + l_i ;$$

$$J = (-g t_p / u_* + k l^+ \Delta W) C(z_0) \text{ for } x_i + l_i \leq x < x_{i+1} .$$

To estimate the aerosol particles dispersion by the turbulent flow the problem (5.16)-(5.17) has been numerically solved for the lead particles of various diameters. The numerical data for the turbulent lead aerosols transport in the Central Sochi is shown in Figure 5.9. The lead aerosol concentration has been normalized on the turbulent concentration scale computed for the aerosol particles fraction with the given diameter $C^* = (q_{pb}^i / u_*) F_a(d) \Delta d$, where $F_a(d)$ is the statistical weight of the particles with diameters in the range $d, d + \Delta d$.

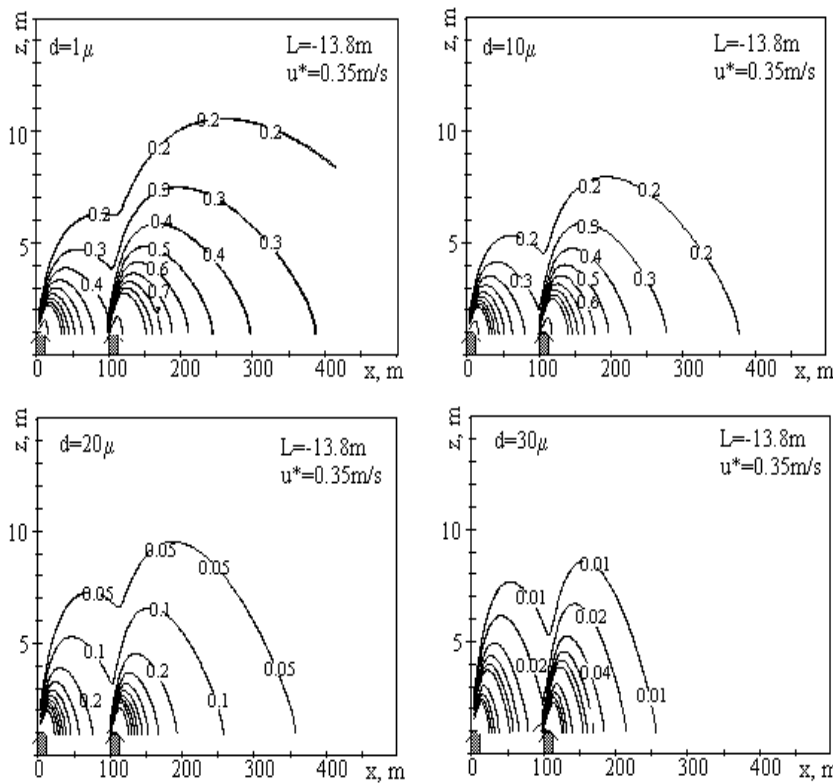


Figure 5.9: Turbulent transport of the lead aerosols of various particles diameter for the fixed meteorological condition. Aerosol concentration is normalized on the turbulent concentration scale computed for the fraction of aerosol particles, $C^* = (q_{Pb}^i / u_*) F_a(d) \Delta d$

As it has been established in the numerical experiments the turbulent diffusion parameters of the particles with diameter less than micron, $d \leq 1\text{m}$, practically independent on their diameter. The differences in the turbulent diffusion parameters are essential for the lead aerosol particles with diameter $d \geq 10\text{m}$.

The heavy particles which have the diameter in the range $d \geq 30\text{m}$ are deposited inside of the 200 m zone. It is well known that the actively polluted space for motorways is about 200 m wide with its main axis coinciding with the motorway main axis [14]. Note, that the air pollutants turbulent transport data shown in Figures 5.7-5.9 agrees with this experimental result.

In the Sochi region in the end of 80's the concentration of lead was higher then the MPC of lead in the air and in soil near the main motorways [2, 13]. In the middle of 90's the environmental situation even more deteriorated in connection with significant increasing of the air pollutants emission. It has been established [13] that the rise of air pollutants emission leads simultaneously to increase the sickness rate of respiratory diseases - see Figure 5.10. Therefore the local administration has forbidden to use the leaded fuel in the Sochi region in

1996. In practice, however, the administrative measures on limitation of the air pollutants emission are not extremely effective, because the total control of exhaust gases is practically impossible to use.

5.2.5. Air pollution impact on human health in the Sochi region

Sochi stretches for 146 km along the Black Sea coast. Only its narrow seaside strip of land, pressed by the main Caucasian mountain range against the Black Sea, is within the city boundaries. The wind rose, the breeze circulation, and the landscape make the air pollutants accumulate and precipitate locally in the Sochi region [14].

Sochi is a seaside climatic Russian resort, thus the air pollution can cause not only the extreme environmental situation in the city, but also the economical crises, because the residential districts as well as the resort institutions are located in the actively polluted zones, rather close to the motorway [2, 13-14]. This obviously affects the state of health of the Sochi residents.

The link between the air pollution and human health in the Sochi area has been established for several diseases as some form of cancer, and asthma [13]. The significant correlation of 0.869 was found between the asthma sickness rate of children (asthma sick per thousand people in year) and the number of vehicles in the Sochi region - see Figures 5.10. The correlation of 0.8158 was found between the Sochi region residents and the number of vehicles - see Figure 5.11.

Note that the correlation of 0.882 between asthma admission and NO_2 level for adults has been reported by Watson et al [134]. Evidently that the people health depends on the air pollutants emission, which in turn is proportional to the number of vehicles.

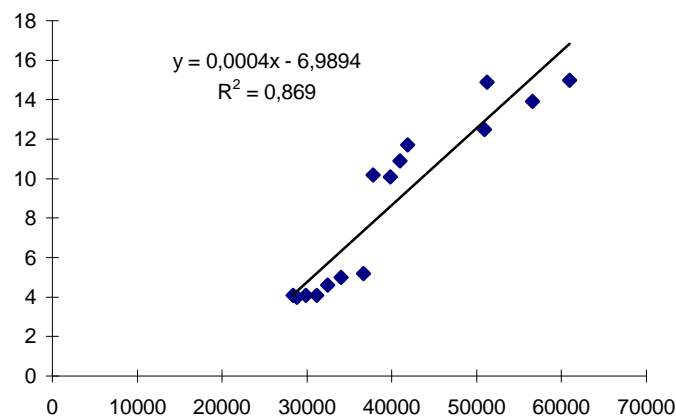


Figure 5.10: Link between the asthma sickness rate of children (asthma sick per thousand in year) and the number of vehicles in the Sochi region [13]

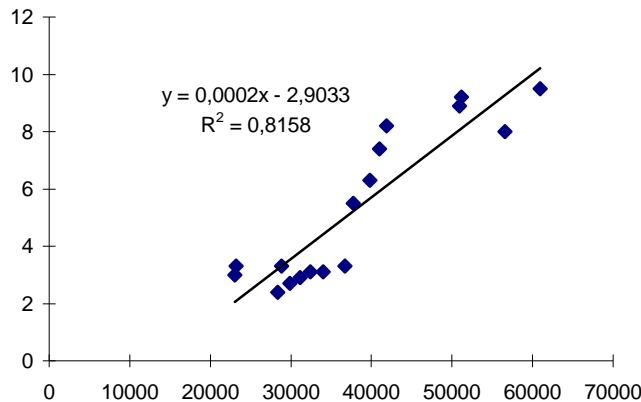


Figure 5.11: Link between the asthma sickness rate of residents (asthma sick per thousand in year) and the number of vehicles in the Sochi region [13]

5.3. Model of aerosols turbulent transport

The mathematical models of the turbulent transport of aerosols in the atmosphere are based mainly on the hypothesis that the eddy diffusivity for the small-sized particles is proportional to the eddy diffusivity of a heat and the latter value is assumed proportional to the eddy viscosity (see Russell et al [135], Meixner et al [136], and other). In turn the turbulent eddy viscosity in the stratified flows is determined from the empirical formulas [23, 24, 26, 27] or from the $k - e$ model [29], or from the turbulent kinetic energy model.

Turbulent boundary layer model considered in the second chapter also can be developed for the case of the atmospheric aerosols transport. This model based on the viscous heat-conducting gas transport equation (2.4) and on the dynamical model of the dust cloud [137]. The aerosol is considered as sets of identical, small-sized particles, which move chaotically under influence of thermal fluctuations and are involved in macroscopic movement together with the air flow. The mass concentration of aerosol particles is considered so small, that the influence of particles to gas dynamic can be neglected. The dynamic parameters of the aerosol particles can be averaged to exclude of the chaotic thermal motion, then its can be described by the continuous functions: the numerical concentration and the aerosol particles flow velocity. Thus at the description of aerosol dynamics we shall take into account the Brownian diffusion, weight and inertia of particles. The motion of mono-disperse small particles in a dust cloud are governed by the transport and momentum equations:

$$\frac{\partial n_p}{\partial t} + \nabla \cdot (n_p \mathbf{u}_p) = D_p \nabla^2 n_p \quad (5.18)$$

$$\frac{\partial \mathbf{u}_p}{\partial t} + (\mathbf{u}_p \cdot \nabla) \mathbf{u}_p = \mathbf{g} + \frac{\mathbf{u} - \mathbf{u}_p}{t_p}$$

Here n_p is the particles numerical density, \mathbf{u}_p is the particles flow velocity vector, D_p is the particle diffusion coefficient.

The diffusion coefficient of the small particles is given by the Einstein's formula: $D_p = k\tilde{T}t_p / m_p$, where $k = 1.38 \cdot 10^{-23}$ J/K is the Boltzmann constant, m_p is the particle mass, t_p is the time relaxation parameter which for the spherical particles in the Stokes' regime is given by $t_p = d_p^2 r_s / 18m$, d_p is the particle aerodynamic diameter, r_s is the particle material density.

Using the transformation method explained in the second chapter, one can derive the equation system for the aerosol turbulent transport as follows

$$\begin{aligned} \frac{\partial \tilde{w}}{\partial h} - h \frac{\partial W_0}{\partial h} &= 0 \\ \frac{\partial \tilde{\mathbf{u}}}{\partial t} + \frac{W}{h} \frac{\partial \tilde{\mathbf{u}}}{\partial h} + \frac{\mathbf{N}}{r_0 h} \frac{\partial \tilde{P}}{\partial h} &= \frac{n}{h^2} \frac{\partial}{\partial h} (1 + n^2 h^2) \frac{\partial \tilde{\mathbf{u}}}{\partial h} - \frac{nn^2 h}{h^2} \frac{\partial \tilde{\mathbf{u}}}{\partial h} + \frac{n\mathbf{N}}{h^2} \frac{\partial W_0}{\partial h} \\ \frac{\partial \tilde{\mathbf{u}}_p}{\partial t} + \frac{W_p}{h} \frac{\partial \tilde{\mathbf{u}}_p}{\partial h} + \frac{\mathbf{N}}{h} \frac{\partial q_p}{\partial h} &= \mathbf{g} + \frac{\tilde{\mathbf{u}} - \tilde{\mathbf{u}}_p}{t_p} \\ \frac{\partial n_p}{\partial t} + \frac{W_p}{h} \frac{\partial \tilde{n}_p}{\partial h} + \frac{\tilde{n}_p}{h} \left(\frac{\partial \tilde{w}_p}{\partial h} - h \frac{\partial W_{0p}}{\partial h} \right) &= \frac{n}{Sc_p h^2} \frac{\partial}{\partial h} (1 + n^2 h^2) \frac{\partial \tilde{n}_p}{\partial h} - \frac{nn^2 h}{Sc_p h^2} \frac{\partial \tilde{n}_p}{\partial h} \end{aligned} \quad (5.19)$$

where $\tilde{\mathbf{u}}_p, \tilde{n}_p$ are the random function of the particles flow velocity and numerical density, accordingly; $W_p = \tilde{w}_p - hW_{0p}$ is the vertical turbulent transport rate of aerosol, $W_{0p} = h_t + h_x \tilde{u}_p + h_y \tilde{v}_p$, $3q_p/2$ is the particles turbulent kinetic energy in the small volume dV_s , $Sc_p = n/D_p$ is the Schmidt number of aerosol.

In case when the aerosol particles are formed due to the condensation from the vapor phase this model can be rewritten as follows

$$\begin{aligned} \frac{\partial \tilde{w}}{\partial h} - h \frac{\partial W_0}{\partial h} &= 0 \\ \frac{\partial \tilde{\mathbf{u}}}{\partial t} + \frac{W}{h} \frac{\partial \tilde{\mathbf{u}}}{\partial h} + \frac{\mathbf{N}}{r_0 h} \frac{\partial \tilde{P}}{\partial h} &= \frac{n}{h^2} \frac{\partial}{\partial h} (1 + n^2 h^2) \frac{\partial \tilde{\mathbf{u}}}{\partial h} - \frac{nn^2 h}{h^2} \frac{\partial \tilde{\mathbf{u}}}{\partial h} + \frac{n\mathbf{N}}{h^2} \frac{\partial W_0}{\partial h} + \frac{\mathbf{g}}{r_0} (\tilde{r} - r_0) \\ \frac{\partial \tilde{T}}{\partial t} + \frac{W}{h} \frac{\partial \tilde{T}}{\partial h} &= \frac{n}{Prh^2} \frac{\partial}{\partial h} (1 + n^2 h^2) \frac{\partial \tilde{T}}{\partial h} - \frac{nn^2 h}{Prh^2} \frac{\partial \tilde{T}}{\partial h} + L_H J_H \end{aligned} \quad (5.20)$$

$$\begin{aligned}
\frac{\partial \tilde{f}}{\partial t} + \frac{W}{h} \frac{\partial \tilde{f}}{\partial h} &= \frac{n}{\mathbf{Sc} h^2} \frac{\partial}{\partial h} (1+n^2 h^2) \frac{\partial \tilde{f}}{\partial h} - \frac{n n^2 h}{\mathbf{Sc} h^2} \frac{\partial \tilde{f}}{\partial h} - J_H \\
\frac{\partial \tilde{\mathbf{u}}_p}{\partial t} + \frac{W_p}{h} \frac{\partial \tilde{\mathbf{u}}_p}{\partial h} + \mathbf{N} \frac{\partial \mathbf{q}_p}{\partial h} &= \mathbf{g} + \frac{\tilde{\mathbf{u}} - \tilde{\mathbf{u}}_p}{t_p} \\
\frac{\partial n_p}{\partial t} + \frac{W_p}{h} \frac{\partial \tilde{n}_p}{\partial h} + \frac{\tilde{n}_p}{h} \left(\frac{\partial \tilde{w}_p}{\partial h} - h \frac{\partial W_{0p}}{\partial h} \right) &= \\
&= \frac{n}{\mathbf{Sc}_p h^2} \frac{\partial}{\partial h} (1+n^2 h^2) \frac{\partial \tilde{n}_p}{\partial h} - \frac{n n^2 h}{\mathbf{Sc}_p h^2} \frac{\partial \tilde{n}_p}{\partial h} + \frac{r_0 J_H}{m_p}
\end{aligned}$$

Here $r_0 c_p L_H$ is the latent heat, $r_0 J_H$ is the rate of the phase transition which depends on the air temperature and vapor pressure as $J_H = J_H(\tilde{T}, p_v)$, $p_v = \tilde{r} f R_v \tilde{T}$, here R_v is the gas constant of the vapor phase.

To estimate the Brownian diffusion effect on the aerosol concentration profile in the turbulent boundary the problem about the aerosol turbulent transport over the industrial region has been solved [48]. As well known the emission for a large industrial region is a periodical function dependent on a daily, weekly and yearly human activity. For simplification let us conjecture that the emission has one maximum during day and one minimum during night, thus

$$q(t) = q_0 + q_1 \cos w(t - t_m),$$

where $q_{0,1}$ are the emission parameters, t_m is the time of the maximal emission, $w = 2\pi / t_d$, t_d is the astronomical day period. Note that the periodical emission function can be found for any large urban area. The main aerosol turbulent transport model in the neutral stratified flow can be derived from the last equation (5.19) used the method explained in section 5.1, hence

$$\frac{\frac{d}{dt} n_p}{\frac{d}{dt} t} = D_p \frac{\frac{d^2}{dt^2} n_p}{\frac{d}{dt} V^2} \quad (5.21)$$

Taken into consideration the particles deposition on the ground rough surface the boundary conditions for the diffusion equation (5.21) can be written as follows

$$\begin{aligned}
z = r &:= w_D n_p - D_p (1 + r^2 / I^2) \frac{\frac{d}{dt} n_p}{\frac{d}{dt} z} = q(t); \\
t_d^{-1} \int_0^{t_d} n_p dt &= N_0
\end{aligned} \quad (5.22)$$

where w_D is the deposition velocity, N_0 is the daily averaged particles numerical density.

The explicit solution of the problem (5.21-5.22) can be written in the form (see [48])

$$\begin{aligned} n_p &= N_0 - \frac{(q_0 - w_D N_0)}{D_p \sqrt{1 + r^2 / I^2}} (V - V_r) + \\ &+ \frac{q_1 \text{Sc}_p \cos J(t, V)}{\sqrt{(w_D \text{Sc}_p + k n_r)^2 + k^2 n_r^2}} e^{-k(V-V_r)} \\ J &= v(t - t_m) - k(V - V_r) - \arctan \frac{k n_r}{k n_r - w_D \text{Sc}_p} \end{aligned} \quad (5.23)$$

where $k = \sqrt{w \text{Sc}_p / 2n}$, $n_r = n \sqrt{1 + r^2 / I^2}$, $V_r = I \operatorname{Arsh}(r / I)$.

The aerosol numerical concentration profiles computed on the equation (5.23) for $t_i = 3, 6, 9, \dots, 24$ h and for $d_p = 2.5$ m, $u_* = 0.1$ m/s are shown in Figure 5.12 (right). The aerosol concentration varies periodically and decreases with height increasing. The characteristic damping length can be estimated from condition $k(V - V_r) \approx 1$, it gives $z_d \approx I \operatorname{sh}[1/kI + \operatorname{Arsh}(r/I)]$. Thus, the aerosol numerical density profiles dependent on the main turbulent scale, $I_0 \approx 8.71n/u_*$, have the maximal damping height.

Using the asymptotic formula $k(V - V_r) \approx kI \ln(z/r)$, for $z \geq d_r \gg I_0$, the concentration profile (5.23) can be simplified as follows

$$n_p = N_0 - \frac{q_0 + w_D N_0}{D_p d_r} I_0^2 \ln \frac{z}{d_r} + N_1 \left(\frac{d_r}{z} \right)^a \cos J \quad (5.24)$$

where $J = v(t - t_m) - a \ln \frac{z}{d_r} - \operatorname{arctg} \frac{k d_r D_p}{k d_r D_p - w_D I_0}$, $a = kI_0$,

$N_1 = q_1 I_0 / \sqrt{(w_D I_0 - k d_r D_p)^2 + (k d_r D_p)^2}$, d_r is the roughness length.

Neglected by the third term in the right part of the first equation (5.24) one can estimate the deposition velocity as

$$w_D = D_p d_r / I_0^2 \ln(H_{\max} / d_r) - q_0 / N_0, \quad (5.25)$$

where H_{\max} is the aerosol penetration maximal height. In the case of zero emission at the normal atmospheric conditions, for the spherical particles and for $H_{\max} / d_r \approx 2 \cdot 10^5$ the equation (5.25) leads to

$$w_D \approx 0.05 u_*^2 d_r / D_p \quad (5.26)$$

Here w_D, u_* [m/s], d_r [m], D_p [m]. This formula is in a good agreement with the experimental data of Garland [138], and Sehemel [139].

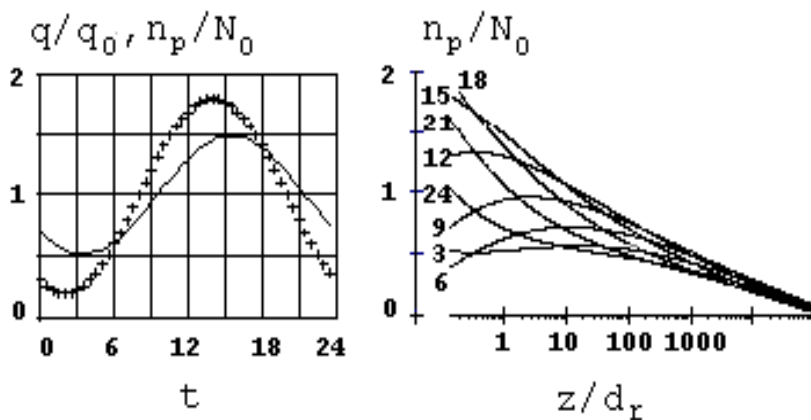


Figure 5.12: On the left side the temporal evaluation of the normalized emission (symbolized line), and aerosol numerical density (solid line); on the right - the normalized aerosol numerical concentration profiles calculated for $t_i = 3, 6, 9, \dots, 24\text{h}$

The aerosol numerical concentration scale in the surface layer can be estimated as

$$N_0 = \frac{q_0 I_0}{k d_r D_p} S(e/e_0, b) \approx \frac{q_0 I_0 n S}{u_* d_r \sqrt{w D_p}} \quad (5.27)$$

$$S = \frac{(e_0/e)^2 - 1}{b + \sqrt{b^2 + [(e_0/e)^2 - 1](1 + b^2)}}$$

Where $e = N_1 / N_0$, $e_0 = q_1 / q_0$, $b = 1 - (kI_0)^{-1} \ln^{-1}(H_{\max} / d_r)$.

Note that the form parameter e in the second equation (5.27) depends on the maximal and minimal aerosol numerical concentration over the ground surface, $e = (N_{\max} - N_{\min}) / (N_{\max} + N_{\min})$. Thus as it follows from the first equation (5.27) the concentration turbulent scale is proportional to the emission and inversely proportional to the turbulent velocity scale.

The temporal evaluation of the normalized emission $q(t) / q_0$ (marked line) and the normalized aerosol numerical density (solid line) over the ground surface computed on the equation (5.24) for $e_0 = 0.8$; $e = 0.6$; $b = 0.95$ are shown in Figure 5.12 (left). As it can be noted, the maximal aerosol numerical density time has a shift from the maximal emission time. This delay depends on the Brownian diffusion parameter and deposition velocity as

$$\Delta t_m = w^{-1} \operatorname{arctg} \frac{k d_r D_p}{k d_r D_p - w_D I_0} \quad (5.28)$$

The minimum of the time shift is for zero deposition velocity $w_D = 0$, and in this case $\Delta t_m = w^{-1}p / 4 = t_d / 8$, hence the maximum of the aerosol concentration is into 3 h after the maximal emission time.

Finally note, that as the Schmidt number for the atmospheric aerosols is a very large, $Sc_p \gg 1$, thus the characteristic damping scale is a very sensitive to the turbulent velocity scale and the aerosol particles size variations. The approximated formula for the damping length can be written as

$$z_d \approx d_r \exp\left(cu_* / \sqrt{d_p}\right), \quad (5.29)$$

Here d_p [m], u_* [cm/s], $c \approx 0.6$.

Therefore in the turbulent atmospheric flow there is a separation of the aerosol particles with height: the small particles penetrate in the high atmospheric layer and the heavy particles move in the bottom layer. But this separation not depends on the gravity acceleration and only on the Brownian diffusion parameter which is inverse proportional to the aerosol particles diameter.

Thus, there are several possibilities to find the Brownian diffusion effect on the aerosol numerical concentration profile (5.23): the maximum concentration time, the aerosol deposition velocity, the particles maximal penetration height and the numerical density scale are dependent on the particles diameter due to the Brownian diffusion.

(To be continued)

References

- [1] Liepmann, H.W., The Rise and Fall of Ideas in Turbulence, *American Scientist*, **67**, pp. 221-228, 1979.
- [2] Amirkhanov, M.M, Lukashina, N.S. & Trunev, A. P., *Natural recreation resources, state of environment and economical and legal status of coastal resorts*, Publishing House "Economics", Moscow, 207 p., 1997 (in Russian).
- [3] Marchuk, G. I., *Mathematical Modelling in the Environmental Problem*, "Nauka", Moscow, 1982 (in Russian).
- [4] Borrell P.M., Borrell P., Cvitas T. & Seiler W., Transport and transformation of pollutants in the troposphere. *Proc. EUROTAC Symp.*, SPB Academic Publishing, Hague, 1994.
- [5] Jaecker-Voirol A., Lipphardt M., Martin B., Quandalle, Ph., Salles, J., Carissimo, B., Dupont, E., Musson-Genon, L., Riboud, P.M., Aumont, B., Bergametti, G., Bey, I., Toupane, G., A 3D regional scale photochemical air quality model - application to a 3 day summertime episode over Paris, *Air Pollution IV. Monitoring, Simulation and Control*, eds. B. Caussade, H. Power & C.A. Brebbia, Comp. Mech. Pub., Southampton, pp. 175-194, 1996.
- [6] Borrego, C., Coutinho, M., Carvalho, A.C.& Lemos, S., A modelling package for air quality management in Lisbon, *Air Pollution V. Modelling, Monitoring and Management*, eds. H. Power, T. Tirabassi & C.A. Brebbia, CMP, Southampton-Boston, pp. 35-44, 1997.

- [7] Bozo, L.& Baranka, G., Air quality modelling over Budapest, *Air Pollution IV. Monitoring, Simulation and Control*, eds. B. Caussade, H. Power & C.A. Brebbia, Comp. Mech. Pub., Southampton, pp. 31-36, 1996.
- [8] Marchuk, G.I. & Aloyan, A.E., Global Admixture Transport in the Atmosphere, *Proc. Rus. Acad. Sci., Phys. Atmosphere and Ocean*, **31**, pp. 597-606, 1995.
- [9] Moussiopoulos N., Air pollution models as tools to integrate scientific results in environmental policy, *Air Pollution III, Vol.1. Theory and Simulation*, eds. H. Power, N. Moussiopoulos & C.A. Brebbia, Comp. Mech. Publ., Southampton, pp.11-18, 1995.
- [10] Pekar M., *Regional models LPMOD and ASIMD. Algorithms, parametrization and results of application to Pb and Cd in Europe scale for 1990*, EMEP/MSC-E Report 9/96, Aug, 78 p., 1996.
- [11] Carruthers, D.J, Edmunds, H.A., McHugh, C.A., Riches, P.J. & Singles, R.J., ADMS Urban - an integrated air quality modelling system for local government, *Air Pollution V. Modelling, Monitoring and Management*, eds. H. Power, T. Tirabassi & C.A. Brebbia, CMP, Southampton-Boston, pp. 45-58, 1997.
- [12] Ni Riain, C., Fisher, B., Martin, C. J. & Littler J., Flow field and Pollution Dispersion in a Central London Street, *Proc. of the 1st Int. Conf. on Urban Air Quality: Monitoring and Modelling*, ed. R. S. Sokhi, Kluwer Academic Publishers, pp. 299-314, 1998.
- [13] Lukashina, N.S. & Trunev, A. P., *Principles of Recreation Ecology and Natural Economics*, Russian Academy of Sciences, Sochi, 273 p., 1999 (in Russian).
- [14] Lukashina, N.S., Amirkhanov, M.M, Anisimov, V.I. & Trunev, A.P., Tourism and environmental degradation in Sochi, Russia, *Annals of Tourism Research*, **23**, pp. 654-665, 1996.
- [15] Lenhart, L. & Friedrich, R. European emission data with high temporal and spatial resolution, *Air Pollution III Vol.2: Air Pollution Engineering and management*, eds. H. Power, N. Moussiopoulos & C.A. Brebbia. Comp. Mech. Publ., Southampton, pp.285-292, 1995.
- [16] Oke, T.R., Street design and urban canopy layer climate, *Energy and Buildings*, **11**, pp. 103-111, 1988.
- [17] Zilitinkevich, S. Non-local turbulent transport: pollution dispersion aspects of coherent structure of convective flows, *Air Pollution III, Vol.1. Air Pollution Theory and Simulation*, eds. H. Power, N. Moussiopoulos & C.A.Brebbia, Comp. Mech. Publ., Southampton, pp.-53-60, 1995.
- [18] Arya, S. P., *Introduction to Micrometeorology*, Academic Press, San Diego, 307 p., 1988.
- [19] Stull, R. B, *An Introduction to Boundary Layer Meteorology*, Kluwer Academic Publishers, Dordrecht, 666 p., 1988.
- [20] Kaimal, J. C.& Finnigan, J. J., *Atmospheric Boundary Layer Flows: Their Structure and Measurements*, Oxford University Press, 289 p., 1994.
- [21] Monin, A.S. & Obukhov, A.M., Basic Laws of Turbulent Mixing in the Atmospheric surface layer, *Trudy Geofiz. Inst. Akad. Nauk SSSR* **24** (151), pp. 163-187, 1954.
- [22] Monin, A. S., The Atmospheric Boundary Layer, *Ann. Rev. Fluid Mech.*, **22**, 1970.
- [23] Businger, J.A., Wyngaard, J.C., Izumi, Y. & Bradley, E.F. Flux Profile Relationships in the Atmospheric Surface Layer, *J. Atmos. Sciences*, **28**, pp.181-189, 1971.
- [24] Businger, J. A., A Note on the Businger-Dyer Profile, *Boundary-Layer Meteorol.*, **42**, pp. 145–151, 1988.
- [25] Yaglom, A.M., Data on Turbulence Characteristics in the Atmospheric Surface Layer, *Izv. Acad. Sci. USSR, Phys. Atmosphere and Ocean*, **10**, pp. 566-586, 1974.
- [26] Dyer, A. J., A Review of Flux-Profile Relationships, *Boundary-Layer Meteorol.*, **7**, pp. 363–372, 1974.
- [27] Van Ulden, A. & Holtslag, A. A. M., Estimation of Atmospheric Boundary Layer Parameters for Diffusion Applications, *J. Clim. Appl. Meteorol.*, **24**, pp. 1196–1207, 1985.
- [28] Hanjalic, K.& Launder, B. E., A Reynolds Stress Model of Turbulence and its Application to Thin Shear Flows, *J. Fluid Mech*, **52**, pp. 609–638, 1972.
- [29] Rodi, W. Calculation of Stably Stratified Shear-layer Flows with a Buoyancy-extended $k - e$ Turbulence Model, *Turbulence and Diffusion in Stable Environments*, ed. J. C. R. Hunt, Clarendon Press, Oxford, pp. 111–143, 1985.
- [30] Mellor, G. L. & Yamada, T. A, Hierarchy of Turbulence Closure Models for Planetary Boundary Layers, *J. Atmos. Sci.*, **31**, pp. 1792–1806, 1974.

- [31] Mellor, G. L. & Yamada, T., Development of a Turbulence Closure Model for Geophysical Fluid Problems, *Rev. Geophys. Space Phys.*, **20**, pp.851–875, 1982.
- [32] Wyngaard, J. C. & Cote, O. R., The Evolution of a Convective Planetary Boundary Layer –a Higher-order-closure Model Study, *Boundary-Layer Meteorol.*, **7**, pp. 289–308, 1974.
- [33] Zeman, O. & Lumley, J. L., Modelling Buoyancy Driven Mixed Layers, *J. Atmos. Sci.*, **33**, pp.1974–1988, 1976.
- [34] Deardorff, J. W. & Willis, G. E., Further Results from a Laboratory Model of the Convective Boundary Layer, *Boundary-Layer Meteorol.*, **32**, pp. 205–236, 1985.
- [35] Enger, L., A Higher Order Closure Model Applied to Dispersion in a Convective PBL, *Atmos. Environ.*, **20**, pp. 879–894, 1986.
- [36] Holt, T. & Raman, S., A Review and Comparative Evaluation of Multilevel Boundary Layer Parameterisations for First Order and Turbulent Kinetic Energy Closure Schemes, *Rev. Geophys. Space Phys.*, **26**, pp. 761–780, 1988.
- [37] Danilov, S.D., Koprav, B. M. & Sazonov, L. A., Atmospheric Boundary Layer and the Problem of Its Description (Review), *Proc. Rus. Acad. Sci., Phys. Atmosphere and Ocean*, **31**, pp. 187-204, 1995.
- [38] Hurley, P. J., An Evaluation of Several Turbulence Schemes for the Prediction of Mean and Turbulent Fields in Complex Terrain, *Boundary-Layer Meteorol.*, **83**, pp. 43–73, 1997.
- [39] Reynolds, O., On the dynamically theory of incompressible viscous fluids and the determination of the criterion, *Philos. Trans. R. Soc. London, A* **186**, 123, 1895.
- [40] Boussinesq, J., Theorie de l'ecoulement tourbillat, *Mem. Pres. Acad. Sci.*, **23**, p. 46, 1877.
- [41] Prandtl, L., Bericht über untersuchungen zur ausgebildeten turbulenz, *Z. Angew. Math. Mech.*, **5**, pp.136-139, 1925.
- [42] Prandtl, L., Neuere Ergebnisse der Turbulenzforschung, *VDI -Ztschr.*, **77**, 5, p.105, 1933.
- [43] Kolmogorov, A.N., The Equations of Turbulent Motion in an Incompressible Fluid, *Izv. Acad. Sci. USSR, Phys.*, **6**, pp. 56-58, 1942.
- [44] Apsley, D. D. & Castro, I. P., A Limited-Length-Scale-Model for the Neutral and Stable-Stratified Atmospheric Boundary Layer, *Boundary Layer Meteorol.*, **83**, pp. 75–98, 1997.
- [45] Trunev, A. P., Diffuse processed in turbulent boundary layer over rough surface, *Air Pollution III, Vol.1. Theory and Simulation*, eds. H. Power, N. Moussiopoulos & C.A. Brebbia, Comp. Mech. Publ., Southampton, pp. 69-76, 1995.
- [46] Trunev, A. P., Similarity theory and model of turbulent dusty gas flow over large-scale roughness, *Abstr. of Int. Conf. On Urban Air Quality: Monitoring and Modelling*, University of Hertfordshire, Institute of Physics, London, p. 3.8, 1996.
- [47] Trunev, A. P., Similarity theory for turbulent flow over natural rough surface in pressure and temperature gradients, *Air Pollution IV. Monitoring, Simulation and Control*, eds. B. Caussade, H. Power & C.A. Brebbia, Comp. Mech. Pub., Southampton, pp. 275-286, 1996.
- [48] Trunev, A. P., Similarity theory and model of diffusion in turbulent atmosphere at large scales, *Air Pollution V. Modelling, Monitoring and Management*, eds. H. Power, T. Tirabassi & C.A. Brebbia, CMP, Southampton-Boston, pp. 109-118, 1997.
- [49] Klebanoff, P. S., Characteristics of turbulence in a boundary layer with zero pressure gradient, *NACA Tech. Note*, **3178**, 1954.
- [50] Laufer, J., The structure of turbulence in fully developed pipe flow, *NACA Tech. Note*, **2954**, 1954.
- [51] Cebeci, T. & Bradshaw, P., *Physical and Computational Aspects of Convective Heat Transfer*, Springer-Verlag, NY, 1984.
- [52] Cantwell, Brian J., Organized motion in turbulent flow, *Ann. Rev. Fluid Mech.*, **13**, pp. 457-515, 1981.
- [53] Kuroda, A., *Direct Numerical Simulation of Couette-Poiseuille Flows*, Dr. Eng. Thesis, the University of Tokyo, Tokyo, 1990.
- [54] Coleman, G.N., Ferziger, J. R. & Spalart, P. R., A numerical study of the turbulent Ekman layer, *J. Fluid Mech.*, **213**, pp.313-348, 1990.
- [55] Trunev, A. P. & Fomin, V. M., Continual model of impingement erosion, *J. Applied Mech. Tech. Phys.*, **6**, pp. 113-120, 1985.

- [56] Trunev, A. P., *Research of bodies erosion distraction in gas flows with admixture particles*, Ph.D. Thesis, Inst. Theoretical and Appl. Mech., Novosibirsk, 1986.
- [57] Nikolaevskii, V.N., The space averaging in the turbulence theory, *Vortexes and Waves*, ed. V.N. Nikolaevskii, Mir, Moscow, pp. 266-335, 1984 (in Russian).
- [58] Landau, L.D. & Lifshitz, E. M., *Hydrodynamics*, 3rd ed., Nauka, Moscow, 1986 (in Russian).
- [59] Pulliam, T. H. & Steger, J. L., Implicit Finite-Difference Simulations of three-dimensional Compressible Flow, *AIAA Journal*, **18**, p. 159, 1980.
- [60] Hirschel, E.H. & Kordulla, W., *Shear Flow in Surface-Oriented Coordinates*, Friedr. Vieweg & Sohn, Wiesbaden, 1986.
- [61] Schlichting, H., *Boundary Layer Theory*, McGraw-Hill, NY, 1960.
- [62] Kutateladze, S.S., *The Wall Turbulence*, Nauka, Novosibirsk, 1973 (in Russian).
- [63] Hairer, E., Norsett, S.P. & Wanner, G., *Solving Ordinary Differential Equations I. Nonstiff Problems*, Springer-Verlag, Berlin, 1987.
- [64] Cantwell, B. J., Coles, D. E. & Dimotakis, P. E., Structure and entrainment in the plane of symmetry of a turbulent spot, *J. Fluid Mech.*, **87**, pp. 641-672, 1978.
- [65] Van Driest, E.R., On turbulent flow near a wall, *J. Aero. Sci.*, **23**, p.1007, 1956.
- [66] Kuroda, A., Kasagi, N. & Hirata, M., A Direct Numerical Simulation of the Fully Developed Turbulent Channel Flow, *Proc. Int. Symp. on Computational Fluid Dynamics*, Nagoya, pp. 1174-1179, 1989.
- [67] Nagano, Y., Tagawa, M. & Tsuji, T., Effects of Adverse Pressure Gradients on Mean Flows and Turbulence Statistics in a Boundary Layer, *Proc. 8th Symposium on Turbulent Shear Flows*, 1992.
- [68] Nagano, Y., Kasagi, N., Ota, T., Fujita, H., Yoshida, H. & Kumada, M., *Data-Base on Turbulent Heat Transfer*, Department of Mechanical Engineering, Nagoya Institute of Technology, Nagoya, DATA No. FW BL004, 1992.
- [69] Smith, R.W., *Effect of Reynolds Number on the Structure of Turbulent Boundary Layers*, Ph.D. Thesis, Princeton University, Princeton, NJ, 1994.
- [70] Kline, S.J , Reynolds, W.C., Schraub, F.A. & Runstadler P.W., The structure of turbulent boundary layers, *J. Fluid Mech.*, **30**, pp. 741-773, 1967.
- [71] Kriklivy, V.V., Trunev, A.P. & Fomin, V.M., Investigation of two-phase flow in channel with damaging wall, *J. Applied Mech. Tech. Phys.*, **1**, pp. 82-87, 1985.
- [72] Trunev, A. P. & Fomin, V.M., Surface instability during erosion in the gas-particles stream, *J. Applied Mech. Tech. Phys.*, **3**. pp. 78-84, 1986.
- [73] Trunev, A. P., Evolution of the surface relief at sputtering by ionic bombardment, *Interaction of nuclear particles with a rigid body*, Moscow, Vol.1, Part 1, pp. 83-85, 1989.
- [74] Blackwelder, R. F. & Eckelmann, H., Streamwise vortices associated with the bursting phenomena, *J. Fluid Mech.*, **94**, pp. 577-594, 1979.
- [75] Nikuradse, J., Strömungsgesetze in Rauhen Rohren, *ForschHft. Ver. Dt. Ing.*, p. 361, 1933.
- [76] Schlichting, H., Experimentelle Untersuchungen zum Rauhigkeits-problem, *Ing.-Arch*, **7**(1), pp.1-34, 1936.
- [77] Bettermann, D., Contribution a l'Etude de la Convection Force Turbulente le Long de Plaques Regueuses, *Int. J. Heat and Mass Transfer*, **9**, p. 153, 1966.
- [78] Millionschikov, M.D., *Turbulent flows in the boundary layer and in the tubes*, Nauka, Moscow, 1969 (in Russian).
- [79] Dvorak, F. A., Calculation of Turbulent Boundary Layer on Rough Surface in Pressure Gradient, *AIAA Journal*, **7**, 1969.
- [80] Dirling, R.B., Jr., A Method for Computing Roughwall Heat-Transfer Rate on Re-Entry Nose Tips, *AIAA Paper*, **73-763**, 1973.
- [81] Simpson, R. L., A Generalized Correlation of Roughness Density Effect on the Turbulent Boundary Layer, *AIAA Journal*, **11**, pp. 242-244, 1973.
- [82] Donne, M. & Meyer, L., Turbulent Convective Heat Transfer from Rough Surfaces with Two-Dimensional Rectangular Ribs, *Int. J. Heat Mass Transfer*, **20**, pp. 583-620 , 1977.
- [83] Coleman, H. W., Hodge, B. K. & Taylor, R. P., A Revaluation of Schlichting's Surface Roughness Experiment, *J. Fluid Eng.*, **106**, pp. 60-65, 1984.
- [84] Clauser, F., The Turbulent Boundary Layer, *Advances in Applied Mechanics*, **4**, pp.1-51, 1956

- [85] Grabov, R. M. & White, C. O., Surface Roughness Effects on Nose Tip Ablation Characteristics, *AIAA Journal*, **13**, pp. 605-609, 1975.
- [86] Sigal, A. & Danberg, J. E., New Correlation of Roughness Density Effect on the Turbulent Boundary Layer, *AIAA Journal*, **25**, pp.554-556, 1990.
- [87] Kind, R. J. & Lawrysyn, M. A., Aerodynamic Characteristics of Hoar Frost Roughness, *AIAA Journal*, **30**, pp. 1703-7, 1992.
- [88] Gargaud, I. & Paumard, G., *Amelioration du transfer de chaleur par l'emploi de surfaces corrugées*, CEA-R-2464, 1964.
- [89] Draycott, A. & Lawther, K.R., Improvement of fuel element heat transfer by use of roughened surface and the application to a 7-rod cluster, *Int. Dev. Heat Transfer*, Part III, pp. 543-52, ASME, NY. 1961.
- [90] Möbius, H., Experimentelle Untersuchung des Widerstandes und der Gschwindigkeitsverteilung in Rohren mit regelmäßig angeordneten Rauhigkeiten bei turbulenter Strömung, *Phys. Z.*, **41**, pp. 202-225, 1940
- [91] Chu, H. & Streeter, V.L., *Fluid flow and heat transfer in artificially roughened pipes*, Illinois Inst. of Tech. Proc., No. 4918, 1949.
- [92] Koch, R., Druckverlust und Wärmeübergang bei verwirbelter Strömung, *ForschHft. Ver. Dt. Ing.*, Series B, **24**, pp. 1-44, 1958.
- [93] Skupinski, E., *Wärmeübergang und Druckverlust bei künstlicher Verwirbelung und künstlicher Wandrauhigkeiten*, Diss. Techn. Hochschule, Aachen, 1961.
- [94] Webb, R. L., Eckert, E.R.G. & Goldstein, R. J., Heat transfer and friction in tubes with repeated-rib roughness, *Int. J. Heat Mass Transfer*, **14**, pp. 601-617, 1971.
- [95] Fuerstein, G. & Rampf, G., Der Einfluß rechteckiger Rauhigkeiten auf den Wärmeübergang und den Druckabfall in turbulenter Ringspaltströmung, *Wärme- und Stoffübertragung*, **2** (1), pp.19-30, 1969.
- [96] Sams, E.W., *Experimental investigation of average heat transfer and friction coefficients for air flowing in circular tubes having square-thread-type roughness*, NACA RME 52 D 17, 1952.
- [97] Fedynskii, O. S., Intensification of heat transfer to water in annular channel, *Problemi Energetiki, Energ. Inst. Akad. Nauk USSR*, 1959 (in Russian).
- [98] Watson, M.A.P., *The performance of a square rib type of heat transfer surface*, CEGB RD/B/N 1738, Berkley Nuclear Laboratories, 1970.
- [99] Kjellström, B. & Larsson, A. E., *Improvement of reactor fuel element heat transfer by surface roughness*, AE-271, 1967, Data reported by Dalle Donne & Meyer (1977).
- [100] Savage, D.W. & Myers, J.E., The effect of artificial surface roughness on heat and momentum transfer, *A.I.Ch.E.J.*, **9**, pp.694-702, 1963.
- [101] Sheriff, N., Gumley, P. & France, J., *Heat transfer characteristics of roughened surfaces*, UKAEA, TRG Report 447 (R), 1963.
- [102] Massey, F.A., *Heat transfer and flow in annuli having artificially roughened inner surfaces*, Ph. D. Thesis, University of Wisconsin, 1966.
- [103] Nunner, W., Wärmeübergang und Druckabfall in rauen Rohren, *ForschHft. Ver. Dt. Ing.*, p. 455, 1956.
- [104] Lawn, C. J. & Hamlin, M. J., *Velocity measurements in roughened annuli*, CEGB RD/B/N 2404, Berkley Nuclear Laboratories, 1969
- [105] Stephens, M. J., *Investigations of flow in a concentric annulus with smooth outer wall and rough inner wall*, CEGB RD/B/N 1535, Berkley Nuclear Laboratories, 1970.
- [106] Perry, A.E. & Joubert, P.N., Rough-Wall Boundary Layers in Adverse Pressure Gradients, *J. Fluid Mech.*, **17**, pp.193-211, 1963.
- [107] Antonia, R.A. & Luxton, R.E., The Response of a Turbulent Boundary Layer to a Step Change in Surface Roughness, Pt. 1. Smooth to Rough, *J. Fluid Mech.*, **48**, pp. 721-762. 1971
- [108] Antonia, R.A. & Wood, D.H., Calculation of a Turbulent Boundary layer Downstream of a Step Change in Surface Roughness, *Aeronautical Quarterly*, **26**, pp. 202-210, 1975.
- [109] Pineau, F., Nguyen, V. D., Dickinson, J. & Belanger, J., Study of a Flow Over a Rough Surface with Passive Boundary-Layer Manipulators an Direct Wall Drag Measurements, *AIAA Paper*, **87-0357**, 1987.

- [110] Osaka, H. & Mochizuki, S., Mean Flow Properties of a d-type Rough Wall Boundary Layer in a Transitionally Rough and a Fully Rough Regime, *Trans. JSME ser. B*, **.55**, pp. 640-647, 1989.
- [111] Byzova, N.L., Ivanov, V.N. & Garger, E.K., *Turbulence in the Atmospheric Boundary Layer*, Leningrad, Hydrometeoizdat, 1989 (in Russian).
- [112] Jackson, P.S., On the displacement height in the logarithmic wind profile. *J. Fluid Mech.*, **111**, pp. 15-25, 1981.
- [113] Wieringa, J., Updating the Davenport Roughness Clarification. *J. Wind Engineer, Industl. Aerodyn.*, **41**, pp. 357-368, 1992.
- [114] Bottema, M., Parameterization of aerodynamic roughness parameters in relation with air pollutant removal efficiency of streets, *Air Pollution III, Vol.2. Air Pollution Engineering and Management*, eds. H. Power, N. Moussiopoulos & C. A. Brebbia, Comp. Mech. Publ., Southampton, pp. 235-242, 1995.
- [115] Kutateladze, S. S., *Similarity Analysis in the Thermal-physics*, Novosibirsk, Nauka, 1982 (in Russian).
- [116] Kim, J., Investigation of Heat and Mass Transport in Turbulent Flows via Numerical Simulation, *Transport Phenomena in Turbulent Flows: Theory, Experiment and Numerical Simulation*, eds. M. Hirata & N. Kasagi, Hemisphere Publishing Corp., Washington, D. C., pp. 157-170, 1988.
- [117] Hogstrom, U., Review of Some Basic Characteristics of the Atmosphere Surface Layer, *Boundary-Layer Meteorol.*, **78**, pp. 215-246, 1996.
- [118] Beljaars, A. C. M. & Holtslag, A. A. M., Flux Parameterization over Land Surfaces for Atmospheric Models', *J. Appl. Meteorol.*, **30**, pp. 327-341, 1991.
- [119] Pugliese, S., Jaeger, M. & Occelli, R., Finite element modelling of plume dispersion in the lower part of the atmosphere, *Air Pollution IV. Monitoring, Simulation and Control*, eds. B. Caussade, H. Power & C.A. Brebbia, Comp. Mech. Pub. Southampton-Boston, 99-108. 1996
- [120] Lui, Jingmiao & Kotoda, Kazuo, Evaluation of Surface-Layer Wind Profiles With Heife Observations, *Boundary-Layer Meteorol.*, **83**, pp. 27-41, 1997.
- [121] Castillo, L., *Similarity analysis of turbulent boundary layers*, Ph. D. Thesis, The Graduate School of the State University of New York, Buffalo, 1997.
- [122] Clauser, F.H., Turbulent boundary layer in adverse pressure gradients, *J. Aeron. Sci.*, **21**, pp. 91-108, 1954.
- [123] Herring, H. & Norbury, J., Some experiments on equilibrium turbulent boundary layers in favourable pressure gradients, *J. Fluid mech.*, **27**, pp. 541-549, 1967.
- [124] Patel, V.C. & Head, M.R., Reversion of Turbulent to Laminar Flow, *J. Fluid. Mech.*, **34**, pp. 371-392, 1968.
- [125] Detering, H. W. & Etling, D., Application of the E- e Turbulence Model to the Atmospheric Boundary Layer, *Boundary-Layer Meteorol.*, **33**, pp. 113-133, 1985.
- [126] Rodi W. Examples of calculation methods for flow and mixing in stratified fluids // *Journal of Geophysical Research.* - 92. - No C5. - 1987. - P. 5305-5328.
- [127] Rodi, W., Examples of Turbulence Models for Incompressible Flows, *AIAA Journal*, **20**, pp. 872-879, 1982.
- [128] Hassan, A. A. & Crowther, J. M., Modelling of fluid flow and pollutant dispersion in a street canyon, *Proc. of the 1st Int. Conf. on Urban Air Quality: Monitoring and Modelling*, ed. R. S. Sokhi, Kluwer Academic Publishers, pp. 281-297, 1998.
- [129] Labatut, A., Cieslik, S., Lamaud, E., Fontan, J. & Druilhet, A., Parameterization of ozone and aerosol particle fluxes, *Air Pollution III, Vol.2. Air Pollution Engineering and Management*, eds. H. Power, N. Moussiopoulos & C. A. Brebbia, Comp. Mech. Publ., Southampton, pp. 141-149, 1995.
- [130] Paltridge, G.W. & Platt, C.M.R., *Radiative processes in meteorology and climatology*, Elsevier Scientific Publication Company, Amsterdam, Oxford, New York, 1976.
- [131] Jenkins, N., Legassick, W., Sadler, L. & Sokhi, R.S., Correlation between NO and NO₂ roadside concentrations, traffic volumes and local meteorology in major London route, *Air Pollution III, Vol.2. Air Pollution Engineering and Management*, eds. H. Power, N. Moussiopoulos & C. A. Brebbia, Comp. Mech. Publ., Southampton, pp. 405-412, 1995.

- [132] Amirkhanov, M.M., Anisimov, V.I., Lukashina, N.S. & Trunev, A. P., Ecological problems of the territorial-recreation complex development of Sochi town, *Izv. Rus. Acad. Sci., Geography*, **1**, pp. 61-71, 1996.
- [133] Francois, Ramade, *Elements d'ecologie appliquee*, Group McGraw-Hill, 1978.
- [134] Watson A.F.R., Barker S., Ardern K.D. An initial investigation into the potential link between air pollution and asthma using geographical information system based technique, *Air Pollution III. V.2, Air Pollution Engineering and Management*, eds. H. Power, N. Moussiopoulos & C. A. Brebbia, Comp. Mech. Publ., Southampton, pp. 447-454, 1995.
- [135] Russell, G., McRae, G. & Cass, G.R., Mathematical Modelling of the Transport of Ammonium Nitrate Aerosol, *Atmospheric Environment*, **17**, pp. 949-964, 1983.
- [136] Meixner, F.X., Franken, H.H., Duijzer, J.H. & Aalst, R.N., Deposition of HNO_3 to a pine forest, *Air Pollution Modelling and its Application VI*, Plenum Press, London, 1988.
- [137] Kiselev, S.P., Ruev, G.A., Trunev, A.P., Fomin, V.M. & Schavaliev, M.S., *Shock-wave phenomena in two-component and two-phase flows*, Nauka, Novosibirsk, 261 p., 1992 (in Russian).
- [138] Garland, J.A., Dry and wet removal of sulphur from the atmosphere, *Atmos. Environ.*, **12**, pp. 349-362, 1978.
- [139] Sehemel, G.A., Particle and gas deposition: a review, *Atmos. Environ.*, **14**, pp. 983-1011, 1980.